# Comparison of Time Base Nonlinearity Measurement Techniques

Gerard N. Stenbakken and John P. Deyst

***Abstract*—Distortions in the timebases of equivalent-time oscilloscopes and digitizers cause distortions of waveforms sampled by them. This paper reports on a comparison of two methods of characterizing timebase distortion, using pure sine-wave inputs of known frequency: the "sinefit" and the "analytic signal" methods. Simulations are used to compare the performance of the two methods versus different types of timebase distortion, different sine-wave frequencies, number of different sine-wave phases, levels of random noise, and levels of random jitter. The performance of the two methods varies considerably, dependent upon the input signal frequency and type of timebase distortion. Each method does much better than the other for certain cases.**

***Index Terms*— Analytic signal, digitizer, distortion, measurement, multiphase, nonlinear, simulation, sinefit, time base.**

## I. Introduction

DISTORTIONS in the timebases of sampling oscilloscopes and waveform digitizers cause distortions of their sampled output. Modern equivalent-time oscilloscopes and digitizers have timebases that are designed to produce a sampling strobe at a known delay after a trigger event. These delays are typically of uniformly increasing duration, resulting in nominally uniformly spaced equivalent-time samples. Timebase distortion is considered here to mean deterministic shifts or deviations in the sample times away from the intended, uniformly spaced, time intervals. (Random shifts of the sample times, also known as jitter or aperture uncertainty, are discussed here but is not the main subject of this paper.)

In the time domain, timebase distortion is manifested in the sampled signal by amplitude errors, to first order, equal to the product of the signal slope and the distortion-induced time shift. In the frequency domain, the effect of timebase distortion is (unwanted) phase modulation of the sampled signal, causing erroneous spectral broadening and/or spurious spectral distortion peaks.

In order to correct for such errors, the timebase distortion first needs to be characterized, so that the actual relative sampling times are known. Using that information, the values of the sampled signal at the nominal sample times can be estimated. In this paper, we only compare methods of accomplishing the first step, the timebase distortion characterization.

Manuscript received June 1, 1997; revised April 1, 1998.

The authors are with the Electricity Division, U.S. National Institute of Standards and Technology, Technology Administration, U.S. Department of Commerce, Gaithersburg, MD 20899 USA (e-mail: stenbakken@eeel.nist.gov).

Publisher Item Identifier S 0018-9456(98)05477-1.

### A. Previous Work

Previous researchers have developed several methods of characterizing timebase distortion, as well as methods of correcting signals for such distortion. In the past, timebases were calibrated using time-mark generators, which are pulse generators driven by stable oscillators. A related timebase calibration source is a circuit that use pulses propagating in a transmission line of known length to produce pulses equispaced in time [1].

Scott and Smith [2] describe a "zero-crossing" distortion characterization method that is related to earlier work [3], [4]. In the zero-crossing method, a pure sine wave of known frequency is input to and sampled by the oscilloscope or digitizer under test (DUT). The output data record is examined, and the points where the sampled sine wave crosses zero (or more generally, crosses its dc offset value) are interpolated. Nominally, these zero-crossings should be equispaced in time; deviations from uniform spacing indicate timebase distortion. The distortion can be estimated by interpolating between these zero-crossing points.

Rettig and Dobos [5] developed methods of analyzing the performance of equivalent-time timebases by inspection of zero-crossings of sampled sine waves having carefully selected frequencies.

The "sinefit" method [6] uses a pure sinewave input of known frequency as the calibration signal. A sinefit (e.g., [7], [8]) is applied to the sampled sine-wave data, and the fit residuals are calculated. The residuals are divided by the calculated derivative of the sinefit, resulting in a timebase distortion estimate. Samples that have phases near the sine-wave peaks are omitted from the division, because of the decreased sensitivity there. Multiple sine waves of different phases are acquired and processed in this way, and the results averaged, to provide estimates of the timebase distortion.

Verspecht [9] developed the "analytic signal" method, based on earlier work [10], [11], that essentially applies digital phase demodulation techniques to the sampled sine-wave data, to estimate the timebase distortion. The method was expanded by Schoukens *et al.* [12] to simultaneously estimate harmonic distortion added by the sampling circuitry or the sine-wave synthesizer, as well as the timebase distortion.

### B. Scope of this Work

In this paper, we have concentrated on comparing the sinefit and analytic signal methods of characterizing timebase distortion, particularly their application to the timebases of equivalent-time oscilloscopes and digitizers.

The zero-crossing method [2] is not included in the comparison because its resolution is sometimes restrictively low, and there is currently no method of improving resolution by combining data from sine waves having different starting phases.

Results of the simulations show the analytic signal method to degrade when there are discontinuities in the timebase distortion, which is a common type of distortion. The sinefit method is shown to become unstable for large timebase distortions and have larger errors for input sinewaves that do not have an integral number of cycles over the sampling record.

## II. Simulation Setup

### A. Simulated System

The system simulated here is an equivalent-time oscilloscope with a timebase having a record length of $N$ samples and a synthesizer producing pure sine waves connected to the oscilloscope sampler and trigger inputs. Note that in real systems, the oscilloscope trigger circuit may not have enough bandwidth to be driven directly by the input sine wave, so it must be driven by a separate synthesizer trigger output that is phase-locked to the sinewave.

### B. Timebase Distortion Models

For this paper we used two models of timebase distortion. One is a sawtooth wave, the other type is a sinusoid superimposed on a ramp, used in previous work [9]. In the experiments we varied the number of sawtooth ramps per sampled record. This can be thought of as varying the "bandwidth" of the timebase distortion (related to phase modulation bandwidth).

To understand why these are appropriate distortion models consider how an equivalent-time oscilloscope or digitizer operates. It samples its input signal at a given time after a trigger event. Typically, such oscilloscopes and digitizers acquire one sample of the repetitive input signal per trigger event (though some equivalent-time instrument timebases can produce multiple samples per trigger event, to speed acquisition [13]). The input signal is thus required to be repetitive in order for it to be measured in this way. To produce the accurate delay after the trigger event, it is common for high-performance equivalent-time oscilloscope timebases to generate a coarse delay, produced by a gated main clock that begins counting at the trigger event, plus a fine delay produced by a Vernier that provides interpolation between integer periods of the main clock. The Vernier can be implemented by a voltage ramp input to a comparator that switches state when the ramp reaches a reference level corresponding to the desired fine delay [5], [14]. (Note that some digitizer timebases avoid the gated main clock and use ramps alone to produce desired delays [15].)

Timebase distortion causes the actual delays from the trigger events to the sample times to be different from the desired delays. Distortion can be caused by startup transients in the gated main clock, mismatch between the main clock period and the fine delay Vernier, or nonlinearity in the fine delay Vernier itself. The actual sample acquisition rate depends on the trigger signal and the oscilloscope, but is typically no faster than a sample per several microseconds, so that the timebase distortion is generally not a function of the previous sample event, but rather of the ability of the timebase to produce the desired delay [5].

A reasonable model of timebase distortion versus sample time, for a typical timebase, depends on the length of the time epoch represented by the sampled signal record. For epochs longer than a main clock period, a model for the timebase distortion might be a long ramp, plus a sawtooth-like periodic or quasi-periodic waveform, plus other possibly periodic features. The long ramp represents the period error of the main clock; the sawtooth, with period equal to that of the main clock, represents the main-clock-versus-Vernier mismatch; and the other periodic features represent Vernier nonlinearity. For shorter time epochs that do not contain the boundary between main clock periods, the distortion model should represent mainly the Vernier nonlinearity, which in experiments and the literature typically appears to vary smoothly [5], [9], [12], [14], [16], [17].

### C. Characterization Method Implementations

For the sinefit algorithm, we mainly followed the procedure in [6]. To save time, we used the nonlinear four-parameter fitting algorithm available in a commercial software package, instead of strictly following any of the procedures in [7].

To make the timebase distortion estimates, a data record, $y[n] = y(nT_s)$, was produced representing sampling of the calibration sine wave, of frequency $f_{\mathrm{cal}}$, by the distorted-timebase oscilloscope. $T_s$ is the sample period. Following the procedure in [6], these data were fit with a sinewave, and data within 15° of the peaks of the fitted sine wave $z[n]$ were excised. Each sample of the fit residual $r[n] = y[n] - z[n]$ is divided by the derivative of the fitted sine wave $z(t)$ at the sample time $nT_s$ to get a distortion estimate $\tau[n]$

$$\tau[n] = \frac{(y[n] - z[n])T_s}{\left.\frac{d}{dt}(z(t))\right|_{t=nT_s}}, \quad n = 0, 1, 2, \cdots, (N-1) \qquad (1)$$

as in [6]. Then, to account for simple scale-factor errors (i.e., errors in the main clock), we added a linear component to the distortion estimate, calculated from the difference between the fit frequency estimate $f_{\mathrm{fit}}$ and the actual calibration sine-wave frequency $f_{\mathrm{cal}}$

$$\tau_{\Delta f}[n] = \tau[n] + nT_s\left(\frac{f_{\mathrm{fit}}}{f_{\mathrm{cal}}} - 1\right). \qquad (2)$$

The sum is the distortion estimate for that data record. The estimates from all the data records, corresponding to different sine-wave starting phases, were averaged to create the final timebase distortion estimate for the sinefit method.

In implementing the analytic signal method, following the practice of [9], we applied a Hamming window to the data before the Fourier analysis and dropped 40 samples from either end of our $N = 500$ timebase distortion estimates after the inverse Fourier analysis.

### D. Simulation Parameters

We ran simulations with various values of the different experimental parameters. We could only test a limited number of the infinite combinations. Some of the parameter value choices were based on a hypothetical measurement setting of a sample period, $T_s = 40$ ps, leading to a 20 ns measurement epoch being defined by the 500-sample record. Note, however, that the results are presented such that they are scalable to other sample periods and measurement epochs.

The following parameters were used in the simulations. Generally, the sawtooth timebase distortion "frequency" was 16 ramps per record, though other rates from 1.2 to 4 ramps per record were analyzed. The other timebase distortion model was a sinusoid plus a ramp as shown in [9, Fig. 1]. This model has 4.5 cycles of sine wave with an amplitude of 20 ps and a ramp that rises by 50 ps over the 500-sample record. Six frequencies of the sine-wave calibration signal were analyzed. These are given in terms of the base frequency $f_{\text{base}}$ which has one cycle across the record. Thus, $f_{\text{base}}$ is given by $f_{\text{base}} = 1/(NT_s)$. The errors in the timebase estimates were determined for one starting phase and the average of 2, 4, and 16 starting phases (one phase used phase 0°, two used 0 and 90°, four used 0, 90, 180, and 270°, and 16 used $0+i360/16°$, $i = 0, 1, \cdots, 15$). Random normally distributed amplitude noise with a zero mean and a standard deviation of 0, 0.1, and 1% of the calibration signal amplitude were used. Normally distributed jitter with a zero mean and a standard deviation of 0, 1, and 10% of the sample period were used.

The examined errors are the differences between the modeled timebase distortion and the distortion as calculated by the two methods. The performance figure of merit is the rms error over the estimates determined by each method.

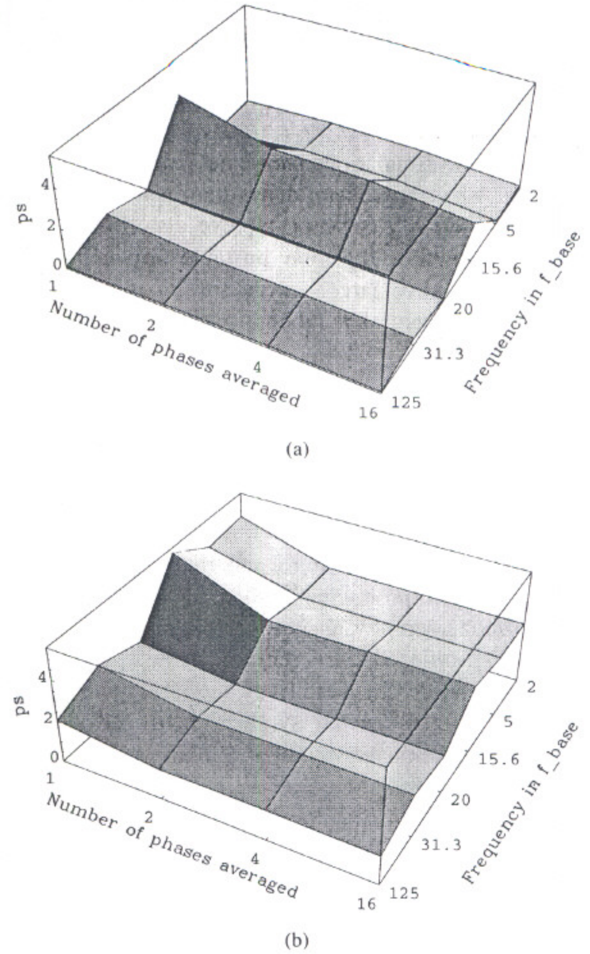


Fig. 1. (a) RMS error in timebase distortion estimate for sinefit method with no noise or jitter and (b) rms error in timebase distortion estimate for analytic signal method with no noise or jitter.

## III. Results

### A. Sawtooth Timebase Distortion Model

Consider first the errors when the modeled timebase distortion is a sawtooth waveform, with exactly 16 ramps across the timebase record. Fig. 1(a) and (b) shows the rms errors in picoseconds for both the sinefit and the analytic signal methods when the sawtooth wave has an amplitude of from $-10$ ps to $+10$ ps. The figures gives results for six different calibration sinewave frequencies, from (2 to 125) $f_{\text{base}}$, and with four different numbers of phases averaged. The most dramatic changes for both methods occur as the calibration signal frequency is varied. These changes are primarily due to the synchronization or lack of synchronization of the calibration signal to the length of the record and to the timebase distortion. The two calibration signal frequencies not synchronized with the record length, 15.6 $f_{\text{base}}$ and 31.3 $f_{\text{base}}$ have the largest errors for both methods. The frequency 15.6 $f_{\text{base}}$ is also close to the frequency of the timebase distortion, 16 $f_{\text{base}}$. Having a calibration frequency equal or nearly equal to the timebase distortion frequency is a poor choice for both methods.

Looking at the cases where both of these methods do best, Fig. 2(a) shows the first 100 samples of the sawtooth timebase distortion and the estimated distortion using the sinefit method with two phases averaged and a calibration frequency of 125 $f_{\text{base}}$. Fig. 2(b) shows a similar plot with the estimated timebase distortion using the analytic signal method with two phases averaged and a calibration frequency of 125 $f_{\text{base}}$. These figures show that the sinefit method more accurately estimates timebase distortions with sharp discontinuities than does the analytic signal method.

The effect of the sawtooth timebase distortion on the sampled values of the calibration signal is to cause discontinuities, as shown in Fig. 3. These discontinuities, as well as calibration signals that are not synchronized with the record, cause spectral leakage [16] in the Fourier analysis used in the analytic signal method, resulting in the larger error values shown in Fig. 1(b). For the sinefit method, these discontinuities primarily result in a shift of the dc offset parameter and, to a smaller extent, an incorrect estimate of the amplitude parameter. Using two calibration signals with approximately 180° phase difference gives equal but opposite shifts in the dc parameter and the same incorrect amplitude estimate. However, since the timebase distortion estimate is dependent on the calibration signal slope and since this is also opposite for a 180° phase shifted signal, the average of these two distortion estimates does not cancel the effects of the dc

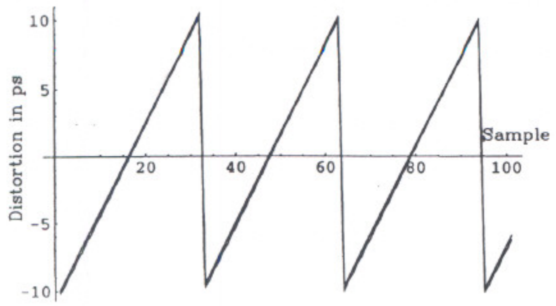


(a)

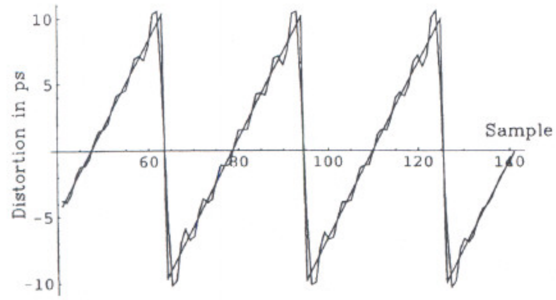


(b)

Fig. 2. (a) Portion of sawtooth distortion and estimate with sinefit method and calibration frequency of 125 $f_{\text{base}}$ and (b) portion of sawtooth distortion and estimate with analytic signal method and calibration frequency of 125 $f_{\text{base}}$.

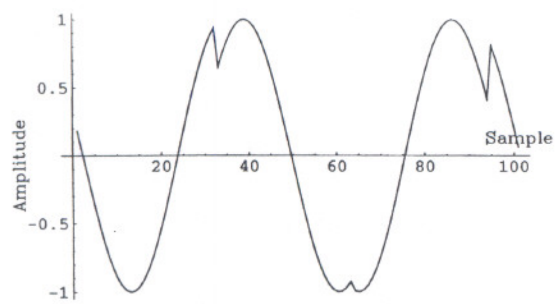


Fig. 3. Discontinuity in sampled sinusoid caused by very large sawtooth timebase distortion.

parameter shift. The effect of the incorrect amplitude estimate is also not canceled. Thus, the averaging of multiple phases will reduce random errors but gives no significant cancellations of dc offset errors or amplitude parameter errors.

For the sinefit method, the largest errors arise when the timebase distortion is repetitive with a frequency approximately equal to the calibration sine-wave frequency, $f_{\text{cal}}$. Stated another way, the largest errors occur when the number of periods of the calibration sine wave in the record is equal to the number of periods of the repetition of the timebase distortion. The sinefit method does best when these two frequencies result in an integer number of cycles across the record, and the two integers have no or few common factors. This happens in the values shown in Fig. 1(a) for the frequencies (2, 5, 20, and 125) $f_{\text{base}}$. For example, the calibration frequency 20 $f_{\text{base}}$ and the timebase distortion frequency of 16 $f_{\text{base}}$ results in

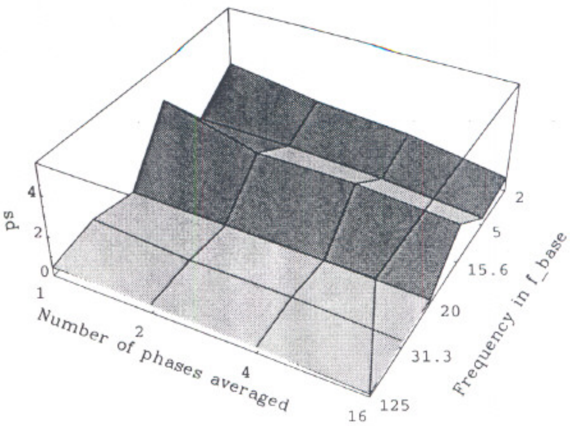


(a)

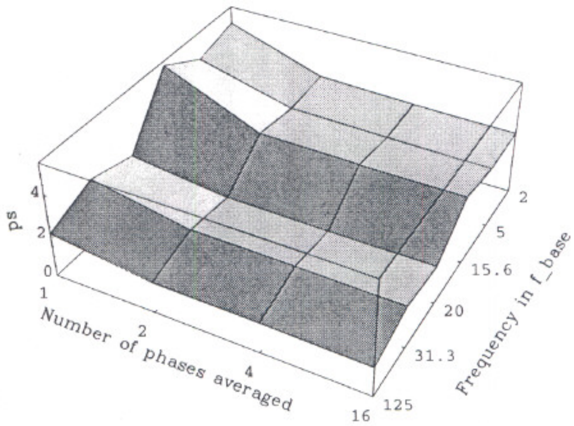


(b)

Fig. 4. (a) RMS error in sawtooth timebase distortion estimate for sinefit method with noise and jitter and (b) rms error in sawtooth timebase distortion estimate for analytic signal method with noise and jitter.

five cycles of the calibration frequency for every four cycles of the timebase distortion. This results in a smaller shift in the dc offset parameter and a more accurate amplitude parameter estimate. This can be seen in Fig. 1(a) as the smaller errors at the frequencies synchronized with the record length and the timebase distortion.

Fig. 4(a) and (b) shows the effects of adding time jitter that is 1% of the sample period as well as noise that is 0.1% of the signal amplitude. For both analysis methods the effect of adding time jitter is to increase the error for all signal frequencies equally. Adding noise increases the error more at lower frequencies than at higher frequencies as can be seen in the figure, and which is predicted from theory.

### *B. Sine Ramp Timebase Distortion Model*

The performance of both methods with a smoothly varying timebase distortion is shown in Fig. 5(a) and (b). The "sine ramp" distortion used in these simulations has 4.5 cycles of a sine wave across the record superimposed on a long ramp [9]. This distortion results in large errors for both methods at low frequencies. For the sinefit method this results from large dc parameter errors for these frequencies. The analytic signal

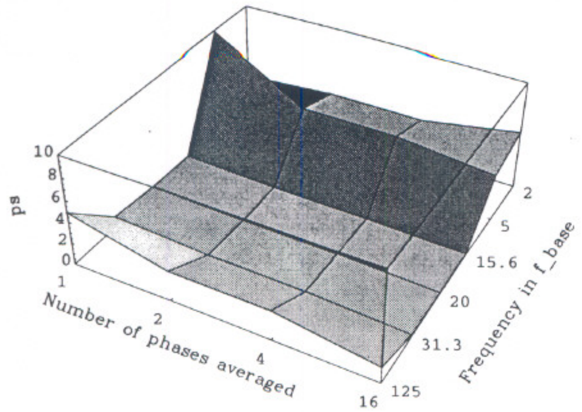


(a)

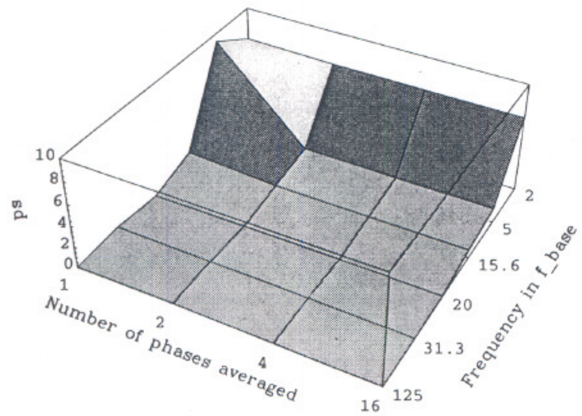


(b)

Fig. 5. (a) RMS error in "sine ramp" timebase distortion estimate for sinefit method with no noise or jitter and (b) rms error in "sine ramp" timebase distortion estimate for analytic signal method with no noise or jitter.

method does poorly when the distortion change is significant during the time the signal is at its peaks as shown by the increase in the errors at lower calibration frequencies. The increase in the errors at the highest frequency, 125 $f_{\mathrm{base}}$, for the sinefit method shows its instability when the phase changes caused by the timebase distortion are large. The errors at this frequency are not proportional to the amplitude of the timebase distortion. For example, when the sine ramp distortion is reduced by a factor of ten, the errors for the sinefit method at this frequency are reduced by a factor of about 100, or to about the same as the errors for the analytic signal method.

### *C. General Results*

The benefit of applying the Hamming window to the sampled data in the analytic signal method is mixed. For the "sine ramp" timebase distortion, the use of the window always reduces the errors in the distortion estimates. For most frequencies the improvement was by a factor of two to three. For the sawtooth timebase distortion, the use of the Hamming window had no effect on the magnitude of the errors of the estimates.

The performance of the sinefit method was unaffected by the number of sawtooth ramps in the timebase distortion, which was varied from 1.2 to 16. However, the distortion-estimate errors for the analytic-signal method increases with the number of ramps. For example, the distortion-estimate errors doubled when the number of ramps was increased from 4 to 16.

The sinefit method excises data that are within 15° of the signal peaks. Increasing this area to 30° or 44° had little effect on the distortion estimate errors. This increase resulted in slightly smaller errors at higher frequencies, 20 $f_{\mathrm{base}}$ and 32 $f_{\mathrm{base}}$, and slightly larger errors at the two lowest frequencies.

## IV. Conclusions

In our simulations, the sinefit method of estimating timebase distortion performs better than the analytic signal method when the timebase distortion has discontinuities, whereas the analytic signal method does better when the timebase distortions are smoothly varying.

The sinefit method performance deteriorated when the timebase distortions were large. This problem occurred for distortion magnitudes greater than about $1/(12\ f_{\mathrm{cal}})$. These large distortions caused phase ambiguities near the peaks of the calibration signal so the error in calculating the signal derivative becomes large. The analytic-signal method showed no such problem for the size of distortions simulated.

The sinefit method has an awkward implementation and requires multiple sine waves of different starting phases to fill the gaps in data where the peaks occur. The analytic-signal method has a simpler implementation and can often perform well using just one calibration sine-wave phase. A disadvantage of the analytic-signal method is that some samples near the ends of the record must be discarded, so the timebase distortion at those samples is not determined.

If noise is significant, both methods performed better with higher calibration frequencies. Note that both methods performed poorly when the timebase distortion was periodic and the calibration sine-wave period was equal, or nearly so, to the distortion period.

Future research includes considering the effect of harmonic distortion and trying an iterative sinefit method.

## Acknowledgment

The authors gratefully acknowledge the help of W. Gans for his advice and comments.

## References

[1] J. R. Andrews, "Pulse measurements in the picosecond domain," Picosecond Pulse Labs Appl. Note AN-3a, p. 2, Oct. 1988.
[2] W. R. Scott, Jr., "Error corrections for an automated time-domain network analyzer," *IEEE Trans. Instrum. Meas.*, vol. IM-35, pp. 300–303, Sept. 1986.
[3] A. M. Nicholson, "Broad-band microwave transmission characteristics from a single measurement of the transient response," *IEEE Trans. Instrum. Meas.*, vol. IM-17, pp. 395–402, Dec. 1968.
[4] W. L. Gans, "Calibration and error analysis of a picosecond pulse waveform measurement system at NBS," *Proc. IEEE*, vol. 74, pp. 86–90, Jan. 1986.
[5] J. B. Rettig and L. Dobos, "Picosecond time interval measurements," *IEEE Trans. Instrum. Meas.*, vol. 44, pp. 284–287, Apr. 1995.
[6] "IEEE Standard for Digitizing Waveform Recorders," IEEE Std. 1057-1994, pp. 46–48, Dec. 1994.

[7] "IEEE Standard for Digitizing Waveform Recorders," IEEE Std. 1057-1994, pp. 17–28, Dec. 1994.
[8] R. Pintelon and J. Schoukens, "An improved sine wave fitting procedure for characterizing data acquisition channels," *IEEE Trans. Instrum. Meas.*, vol. 45, pp. 588–593, Apr. 1996.
[9] J. Verspecht, "Accurate spectral estimation based on measurements with a distorted-timebase digitizer," *IEEE Trans. Instrum. Meas.*, vol. 43, pp. 210–215, Apr. 1994.
[10] Y.-C. Jenq, "Digital spectra of nonuniformly sampled signals: A robust sampling time offset estimation algorithm for ultra high-speed waveform digitizers using interleaving," *IEEE Trans. Instrum. Meas.*, vol. 39, pp. 71–75, Feb. 1990.
[11] A. Papoulis, *Probability, Random Variables, and Stochastic Processes.* New York: McGraw-Hill, pp. 181, 357.
[12] J. Schoukens, R. Pintelon, and G. Vandersteen, "A sinewave fitting procedure for characterizing data acquisition channels in the presence of time base distortion and time jitter," in *IEEE IMTC/96 Conf. Dig.*, Brussels, Belgium, June 4–6, 1996, pp. 1419–1424.
[13] T. M. Souders, B. C. Waltrip, O. B. Laug, and J. P. Deyst, "A wideband sampling voltmeter," in *IEEE IMTC/96 Conf. Dig.*, Brussels, Belgium, June 4–6, 1996, pp. 1139–1144.
[14] J. Verspecht, "Calibration of a measurement system for high frequency nonlinear devices," Ph.D. dissertation, Vrije Univ. Brussel, Brussels, Belgium, pp. 38–41, Sept. 1995.
[15] C. Gyles, "Repetitive waveform high frequency, high precision digitizer," *IEEE Trans. Instrum. Meas.*, vol. 38, pp. 917–919, Aug. 1989.
[16] F. J. Harris, "On the use of windows for harmonic analysis with the discrete Fourier transform," *Proc. IEEE,* vol. 66, pp. 51–83, Jan. 1978.
[17] W. L. Gans, unpublished experimental data and comments, Jijit Metrology, LLC, Feb. 1997.

**Gerard N. Stenbakken** received the Bachelor of physics degree from the University of Minnesota, Minneapolis, in 1964, the M.S. degree in physics from the University of Maryland in 1969, and the M.S. degree in electrical engineering from the University of Maryland, College Park, in 1986.

From 1963 to 1969, he worked with Vitro Laboratories, Silver Spring, MD. In 1969, he joined the National Bureau of Standards (now the National Institute of Standards and Technology), Gaithersburg, MD. There, he worked on semiconductor devices measurement methods, designed a wideband power measurement standard, developed methodologies and software tools for reducing the cost of testing complex electronic devices, and modeled the magnetic field of the electrical based kilogram apparatus.

**John P. Deyst** received the B.S. and M.S. degrees in electrical engineering from the Massachusetts Institute of Technology, Cambridge, in 1988 and 1990, respectively.

Since the beginning of 1993, he has worked at the U.S. National Institute of Standards and Technology, Gaithersburg, MD, on characterizing waveform sampling systems and precision signal sources.

Mr. Deyst serves on the IEEE TC-10 Waveform Measurements and Analysis Committee.

IEEE TRANSACTIONS ON

# INSTRUMENTATION AND MEASUREMENT

A PUBLICATION OF THE IEEE INSTRUMENTATION AND MEASUREMENT SOCIETY

FEBRUARY 1998 VOLUME 47 NUMBER 1 IEIMAO (ISSN 0018–9456)

## SPECIAL ISSUE ON SELECTED PAPERS IMTC'97



*(Continued on page 1)*